Time Course of Electrical Impedance During Red Blood Cell Aggregation in a Glass Tube: Comparison With Light Transmittance

Oguz K. Baskurt*, Mehmet Uyuklu, and Herbert J. Meiselman

***Abstract*—Red blood cells (RBC) in normal human blood undergo reversible aggregation at low flow or stasis. The extent and kinetics of this phenomenon have been studied using various optical and electrical methods, yet results using such methods are not always in concordance. This study employed a horizontal glass tube in which blood flow could be established, then abruptly stopped. Normal blood and RBC suspensions with enhanced or decreased aggregation were studied. Light transmittance (LT) and electrical impedance at 100 kHz were recorded during high-shear flow and for 120 s after flow was abruptly stopped during which RBC aggregation occurs. Capacitance values were also obtained based on the imaginary part of impedance data and recorded. Various aggregation parameters were calculated, using the time course of LT, impedance, and capacitance, then compared with each other and with results from laboratory aggregometers. RBC aggregation parameters were calculated, using the time course of impedance data often failed to correlate with known changes of aggregation, even reporting aggregation for cells in nonaggregating media (i.e., RBC in buffered saline). Alternatively, RBC aggregation parameters based upon the time course of capacitance data are in general agreement with those derived from LT data and with RBC aggregation indexes, measured using commercial instruments.**

***Index Terms*—Capacitance, impedance measurement, light transmittance (LT), red blood cell (RBC) aggregation.**

I. Introduction

THE ELECTRICAL properties of red blood cell (RBC) suspensions have been the subject of numerous investigations, most of which were aimed at developing rapid diagnostic methods [1]–[4]. The studies using electrical impedance and dielectric spectroscopy methods indicated that both the resistive and capacitive properties of blood are determined by the electrical characteristics of plasma (i.e., the suspending phase of blood) and of RBC [5], [6]. Detailed theoretical analyses of the electrical properties of RBC suspensions exist in the literature [7]–[10].

Plasma and the fluid within RBC (i.e., concentrated hemoglobin solution) have different conductivities [5], and these two fluid compartments are separated from each other by the RBC membrane, which has a very low electrical conductivity but introduces capacitance into the system [5]. These factors can be lumped into a three-element model of blood impedance [11] that includes plasma resistance (R_p), internal resistance of the RBC (R_i), and RBC membrane capacitance (C_m) (see Fig. 1). The volume fraction of RBC in blood (hematocrit) and the shape of RBC have been identified as important determinants of their relative contribution to the equivalent impedance, and hence, the measured electrical parameters of blood samples [5], [9], [12]. The resistivity of blood (ρ_b) can be estimated, using plasma resistivity and hematocrit by various approaches [13], [14], including the well-known Maxwell–Fricke equation

$$\rho_b = \rho_p \frac{1 + kH}{1 - H} \tag{1}$$

where ρ_p is plasma resistivity, H is hematocrit, and k is a factor depending on the geometry and orientation of RBC.

The electrical properties of RBC suspensions depend on whether they are flowing or at stasis [8], [9], and Hoetink *et al.* [9] have theoretically analyzed the flow dependence of blood's electrical conductance in a cylindrical tube in detail. Their theoretical work is based on the Maxwell–Fricke theory (1), and therefore, strongly depends on factors related to RBC geometry and orientation. These factors are determined by the applied shear forces during flow and by cellular mechanical properties (i.e., RBC deformability) [15]. Since the theoretical results of Hoetink *et al.* agreed well with experimental data, they thus concluded that the flow dependence of conductance can be explained by RBC orientation and deformation [9]. However,

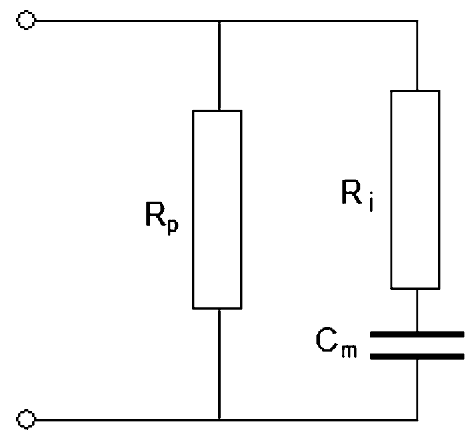

Fig. 1. Three element model of blood impedance. R_p, R_i, and C_m.

Manuscript received July 23, 2009; revised October 5, 2009. First published November 20, 2009; current version published March 24, 2010. This work was supported in part by the National Institutes of Health Research under Grants HL15722, HL 70595, and HL 090511 and in part by the Akdeniz University Research Projects Unit. *Asterisk indicates corresponding author*.

*O. K. Baskurt is with the Department of Physiology, Faculty of Medicine, Akdeniz University, Antalya 07070, Turkey (e-mail: baskurt@akdeniz.edu.tr).

M. Uyuklu is with the Department of Physiology, Faculty of Medicine, Akdeniz University, Antalya 07070, Turkey (e-mail: uyuklu@akdeniz.edu.tr).

H. J. Meiselman is with the Department of Physiology and Biophysics, Keck School of Medicine, Los Angeles, CA 90033 USA (e-mail: meiselma@usc.edu).

Color versions of one or more of the figures in this paper are available online at http://ieeexplore.ieee.org.

Digital Object Identifier 10.1109/TBME.2009.2036598

0018-9294/$26.00 © 2009 IEEE
Authorized licensed use limited to: Bezm-i Alem Universitesi. Downloaded on September 22,2025 at 11:42:42 UTC from IEEE Xplore. Restrictions apply.

these theoretical models ignore cellular aggregation, another important aspect of RBC rheological behavior, which significantly affects the effective particle geometry during shear flow or at stasis [16].

RBC form multicellular aggregates at stasis or when subjected to low shear forces [17]. This reversible aggregation is characterized by a special structure, with RBC–RBC contact forming parallel surfaces like a stack of coins, a process that is frequently termed rouleaux formation. Certain plasma proteins (e.g., fibrinogen) are necessary for RBC aggregation, and therefore, rouleaux formation does not take place in suspensions without these proteins (e.g., isotonic saline). RBC aggregation can also be induced by polymers (e.g., dextrans) of appropriate molecular weight [16], [17]. The degree of RBC aggregation is also determined by the shear forces affecting these cells; therefore RBC aggregates dominate under low shear forces or at stasis. RBC aggregation is an important determinant of the flow properties of blood, especially under low flow conditions [17], has a significant potential to adversely affect *in vivo* blood flow and tissue perfusion [16], [18], and is enhanced during certain pathophysiological processes (e.g., inflammatory processes). RBC aggregation is accepted as a clinically important parameter [19].

Various approaches have been utilized to assess RBC aggregation, ranging from simply observing the erythrocyte sedimentation rate (ESR) over an hour period [20] to more detailed analysis by monitoring light reflectance (LR) or transmittance (LT) from or through RBC suspensions [21]–[26]. Previous studies have simultaneously monitored LT and microscopically observed RBC aggregation and report a strong correlation during the time course of aggregation [27], thus making LT methods accepted by workers in the field [20]. The time course of LR following a sudden stop of blood flow is known as a syllectogram and reflects the time course of aggregation [26]. LT-time data are also termed syllectograms. Both LR and LT syllectograms can be mathematically analyzed to determine various indexes and/or time constants to quantitate RBC aggregation [21], [23], [28], and there are commercially available instruments based on monitoring LT or LR [29].

It has been recognized that RBC aggregation affects the electrical properties of native blood and RBC suspensions [5], [6], [30]–[34]. While some observations reflect changes due to aggregation prior to the start of a measurement (i.e., RBC aggregation occurring before collecting data) [5], [6], [31], others have investigated the potential of electrical impedance derived parameters to quantitate the process of RBC aggregation [30], [32]–[34]. The time course of electrical impedance or conductance has been reported to be similar to LT or LR; therefore suggesting that electrical changes provide the same information regarding aggregation kinetics [30], [34]. However, previous studies have not directly examined this suggestion via a direct comparison of the time course of electrical properties with LT or LR data that are widely accepted to reflect the time course of aggregation [21]–[23], [26]. In addition, previous observations have revealed an unexpected finding: electrical impedance has a syllectogram-like time course for nonaggregating RBC suspensions that is similar to that observed for aggregating RBC suspensions (e.g., RBC in plasma) [35].

This study was designed to compare the time course of electrical impedance and derived capacitance with that for LT during RBC aggregation in a horizontal glass tube. RBC suspended in nonaggregating and aggregating media were investigated; comparisons between measured modalities were based on calculated aggregation indexes that are accepted to reflect RBC aggregation [20], [36] and are used by commercial instruments [23].

II. Materials and Methods

A. Blood Samples and RBC Suspensions

Venous blood samples were obtained from healthy human male volunteers, aged from 25 to 52 years, and anticoagulated with sodium heparin (15 IU/ml). The blood was centrifuged at 1400 g for 5 min, and the plasma carefully aspirated and saved. For some experiments, plasma was diluted with phosphate buffered saline (PBS; pH $= 7.4$, osmolality 290 ± 5 mOsm/kg) at a ratio of 1/2 and 1/3, corresponding to 50% and 66% of original plasma components. RBC from each donor were resuspended either in unmodified or diluted plasma at a hematocrit of 0.4 l/l. RBC were also resuspended in PBS containing 1% bovine serum albumin at 0.4 l/l; albumin does not cause aggregation and maintains the normal resting RBC shape. For some experiments, dextran 500 (MW $=$ 500 kDa, D-5251, Sigma Chemical Company, St. Louis, MO) was dissolved in undiluted plasma at a concentration of 1% and RBC from each donor were resuspended in the plasma + dextran media at 0.4 l/l hematocrit. Compared to cells in undiluted plasma, RBC suspended in diluted plasma exhibit reduced aggregation due to lower concentrations of plasma proteins (e.g., fibrinogen), which induce aggregation [37], while RBC in plasma containing 1% dextran 500 (a strong RBC aggregator) are characterized by enhanced aggregation [38]. Note that while most experiments were done at a hematocrit of 0.40 l/l, some experiments employed 0.30 and 0.50 l/l hematocrits, with all hematocrits determined, using the microcapillary method (i.e., 12000 g for 5 min); hematocrits were adjusted by adding or removing the appropriate suspending medium. All experiments were completed within 4 h after blood sampling [36].

B. Characterization of RBC Aggregation

RBC aggregation indexes for the final RBC suspensions were determined, using two commercially available instruments: 1) a cone-plate photometric aggregometer (Myrenne Aggregometer, Myrenne Gmbh, Roetgen, Germany) [24] employing LT was used to measure a dimensionless aggregation index (M) obtained at stasis after abrupt stoppage of shear; and 2) a Couette aggregometer using a system based on laser light-backscattering (LORCA, RR Mechatronics, Hoorn, The Netherlands) [23]. All aggregation measurements were conducted at 37 °C.

C. Experimental System

The experimental system used for the LT and electrical measurements is shown schematically in Fig. 2. The electrical

Authorized licensed use limited to: Bezm-i Alem Universitesi. Downloaded on September 22,2025 at 11:42:42 UTC from IEEE Xplore. Restrictions apply.

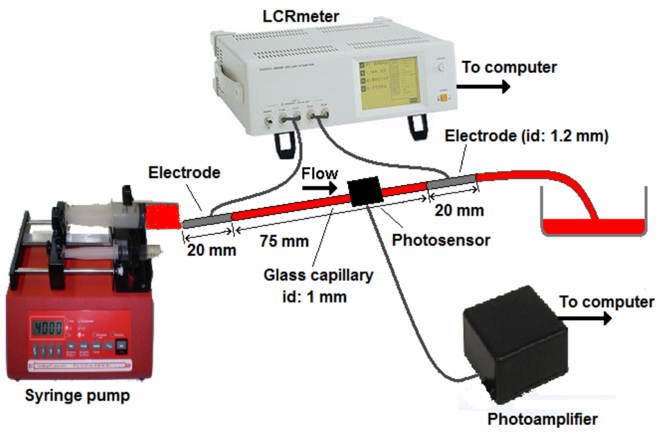

Fig. 2. Schematic representation of the measurement system. The glass tube was horizontal with the axis of the LED-photometer horizontal and perpendicular to the axis of the tube.

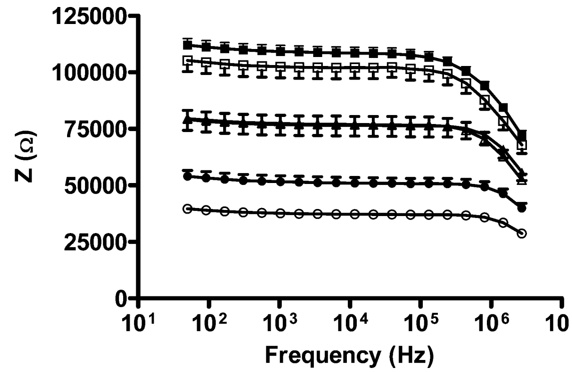

Fig. 3. Z of the glass tube filled with RBC suspended in undiluted plasma during flow (□) and after 120 s after flow stoppage (■) as measured at frequencies between 42 Hz and 2.7 MHz. Z values of the glass tube filled with RBC suspended in PBS measured during flow (△) and at stasis (▲) are also shown. The hematocrit was 0.4 l/l for all suspensions. Also shown are impedance data for cell-free PBS (○) and undiluted plasma (●) at stasis. Data as mean ± standard deviation, $n = 8$.

and LT properties of RBC suspensions were simultaneously recorded in a horizontal glass tube (1 mm ID and 75 mm length) during and after the stoppage of flow induced by a syringe pump (Model NE1000, New Era Pump Systems, Inc., Wantagh, NY). Two stainless-steel tubes (OD: 1.65 mm, ID: 1.19 mm, and length: 20 mm) were attached to each end of the tube to serve as electrodes for electrical measurements and were also used as hydraulic connections to the flow system. These electrodes were connected to a LCR (inductance, capacitance, and resistance) meter (Hioki, 3532-50LCR HiTester, Nagano, Japan) for measurement of electrical impedance and derived parameters. A two-electrode approach was used for the measurements [31] with the instrument controlled by a digital computer via an RS-232 connection. The instrument was run in a series equivalent circuit mode. The LCR meter applies a test signal across the electrodes at a selected frequency and a constant voltage (V), measures the resulting current (I), and phase angle (θ) between V and I. Impedance (Z) is calculated as V/I, while reactance (X) is calculated as $|Z|\cdot\sin\theta$. Series capacitance (C) is then calculated as $1/\omega X$, where ω is the angular velocity corresponding to the test frequency [39]. The signal voltage was held constant at 1 V, resulting in currents in the order of 10^{-5} amp through the tube filled with the RBC suspensions. The results of 16 measurements were averaged by the instrument and reported as a single data point.

The frequency of the test signal was selected based on preliminary studies. Fig. 3 presents the impedance spectrum of RBC suspended in plasma and PBS during flow and at 120 s following flow stoppage (i.e., after full development of RBC aggregates). These results indicated that the difference between flowing and stagnant (i.e., aggregated) RBC suspensions in plasma was not frequency dependent for low frequencies, including the beginning of the β-dispersion range (i.e., ~100 kHz) [40]. C values under similar testing conditions were found to be strongly dependent on frequency, decreasing by about 10^3 as the frequency changed from the lowest (42 Hz) to about 100 kHz (data not shown).

It should be noted that the difference between Z values during flow and stasis of RBC suspension in PBS was negligible except at highest range of measurement frequencies (see Fig. 3). RBC aggregation requires the presence of certain plasma proteins (e.g., fibrinogen) or high-molecular weight polymers (e.g., dextrans), and hence, RBC suspensions in PBS exhibit no detectable aggregation. As the RBC suspensions in PBS and plasma were otherwise the same, the difference of Z between flowing and stagnant RBC suspensions in plasma reflects the influence of fully developed aggregation at 120 s.

The two levels of Z values for RBC suspensions in plasma mentioned earlier (during flow or at stasis; Fig. 3) reflect two specific conditions: no RBC aggregation (i.e., during flow) or complete aggregation (i.e., at stasis, 120 s after flow stoppage). However, previous experiments indicated that electrical values during the aggregation process (i.e., during the 120 s period after flow stoppage) may exceed the values corresponding to flow and to complete aggregation, owing to the initial phase after flow stoppage [35]. The amplitude of Z and C changes during the transition from flow to the stasis (i.e., full development of aggregation process) was maximum at 100 kHz. C values were most stable at this frequency, but exhibited large temporal fluctuations if measured at lower frequencies, possibly reflecting shear rate dependent electrode effects, which may be influenced by shear forces during flow and the transition phase to stasis. Therefore, based on these preliminary experiments, 100 kHz was selected as the frequency of the test signal. This frequency yields the largest β-dispersion effect primarily reflecting the capacitive effects of cell membranes [40] and has been previously recommended for measuring the electrical parameters of blood [32]. The stray capacitance and inductance of the system were tested according to Pribush *et al.* [32] and were found to be negligible.

To monitor LT through the glass tube a phototransistor and an infrared LED (850 nM) were placed opposite to each other at the middle of the glass tube with their axis horizontal and perpendicular to the axis of the tube (see Fig. 2). The signal from the phototransistor was transferred to an amplifier, then

Authorized licensed use limited to: Bezm-i Alem Universitesi. Downloaded on September 22,2025 at 11:42:42 UTC from IEEE Xplore. Restrictions apply.

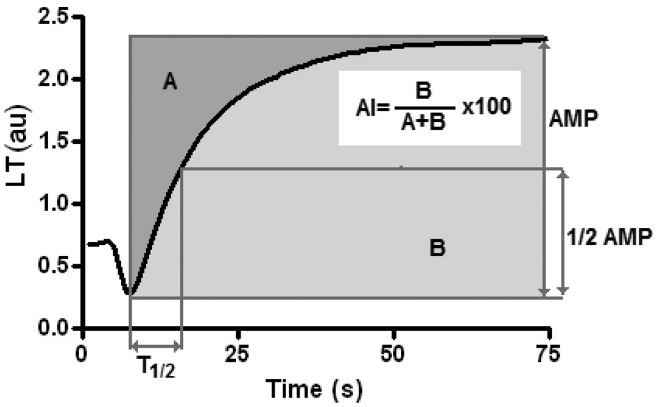

Fig. 4. Calculation procedure for aggregation parameters, using LT-time data. "A" and "B" are the areas of the surfaces above and below the curve, respectively. AI is equal to B/(A + B) and SA is equal to B.

digitized and stored on a computer simultaneously with electrical parameters.

D. Experimental Protocol

For recordings during flow, the syringe pump was run at a volumetric flow rate of 42 ml/min, resulting in a nominal average shear rate of about 500 s^{-1}, this shear rate has been shown to exceed that needed for complete dispersion of all RBC aggregates [20], [41]. After assuring stable conditions the pump was turned off, thereby abruptly stopping flow. *Z*, *C*, and LT were recorded simultaneously at 1 Hz sampling frequency for 5 s during flow and for 120 s following the sudden stoppage of flow. The flow system, including the glass tube, electrodes and LT detector unit were placed in a temperature-controlled box and maintained at 37 °C.

E. Calculations and Statistics

LT, *Z*, and *C* data recorded during the aggregation process after abruptly stopping flow were used to calculate aggregation parameters; surface area (SA), aggregation index (AI), and aggregation half-time ($T_{1/2}$), which are equivalent to those reported by commercially available LT or LR RBC aggregometers [23], [28], [42]. The first 75 s period following stoppage of flow was analyzed, using software written in LabView 8.6 (National Instruments, Austin, TX), as the alterations in the last 45 s of the recorded data had no significant effect on the calculated parameters, using *Z* and *C* time courses, while sedimentation of RBC may start to affect the time course of LT during this late phase. Fig. 4 indicates how the SA, AI, and $T_{1/2}$ parameters are obtained when using LT data. The calculation starts with the determination of a minimum, which corresponds to the completion of RBC shape recovery after the sudden stoppage of flow [23]. This is followed by a characteristic increase of LT reflecting the time course of aggregation. The SA parameter is the area below the curve (B in Fig. 4), while AI corresponds to the ratio of the area under the curve B to the sum of areas below and above the curve (A + B). $T_{1/2}$ is the time required to reach one-half of the total change in LT during 75 s. Since the directions of *Z* and *C* changes due to RBC shape recovery and aggregation were opposite to those for LT (see Fig. 6), the positive peak was taken as the start of calculations for electrical recordings. The calculations were otherwise similar to those for LT except that SA corresponds to the area above the curve, and AI was calculated as the ratio of the area above the curve to the sum of areas under and above the curve. Note that the Myrenne aggregometer yields an "M" parameter, using the same approach as the SA parameter described earlier [24].

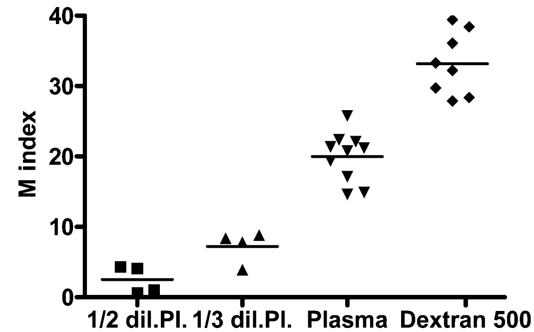

Fig. 5. M for RBC suspended in 1/3 and 1/2 diluted plasma, undiluted plasma and plasma containing 1% dextran 500 kDa dextran (D500). The horizontal line for each group represents mean value.

Data are presented as mean ± standard error (SE). Pearson correlation coefficients and linear regression models were employed to evaluate relationships between parameters calculated using different modalities (i.e., LT, *C*, or *Z*) reflecting the same aggregation processes, as well as those between these parameters and aggregation indexes measured using the RBC aggregometers.

III. Results

A. Aggregation Characteristics of RBC Suspensions

The four types of RBC suspensions used herein exhibited different aggregation characteristics as indicated by the Myrenne aggregometer "M" index (see Fig. 5). Mean values of M were 2.5 ± 1.0, 7.2 ± 1.1, 19.9 ± 1.1, and 33.2 ± 1.6 for 1/2 diluted, 1/3 diluted, undiluted, and dextran-containing plasma suspensions, respectively. In addition to the M index measured by Myrenne aggregometer, parameters provided by the laser-assisted optical rotational cell analyzer (LORCA) laser backscattering aggregometer, which employs a mathematical approach consistent with that used in this study (see Fig. 4), also revealed significant differences between the RBC suspensions (see Table I). Note the marked increases of SA and AI, and the progressive decrease of $T_{1/2}$ with increased RBC aggregation (i.e., 1/2 diluted plasma to 1/3 diluted plasma to plasma to plasma +1% dextran 500 kDa). In particular, the kinetics of aggregation as indexed by $T_{1/2}$ are greatly affected, a ten-fold change of $T_{1/2}$ versus a 3- to 4-fold change for SA and AI for the range of aggregation shown in Table I.

B. Electrical Characteristic of RBC-plasma Suspensions

The *Z* and *C* of RBC suspensions in undiluted plasma measured during flow sufficient for complete dispersion of RBC

Authorized licensed use limited to: Bezm-i Alem Universitesi. Downloaded on September 22,2025 at 11:42:42 UTC from IEEE Xplore. Restrictions apply.

TABLE I
AGGREGATION PARAMETERS REFLECTING EXTENT AND DYNAMICS OF RBC AGGREGATION MEASURED USING LORCA AGGREGOMETER. (PLEASE SEE SECTION II-E FOR DEFINITION OF PARAMETERS)

		SA	AI	$T_{1/2}$
1/2 diluted plasma	(n=4)	16.8 ± 4.5	20.2 ± 1.6	17.8 ± 1.8
1/3 diluted plasma	(n=4)	34.4 ± 6.4	34.6 ± 4.4	8.4 ± 1.9
Plasma	(n=10)	51.3 ± 4.7	63.9 ± 2.3	2.2 ± 0.2
Plasma + 1% D500	(n=8)	58.51 ± 5.3	69.4 ± 0.3	1.7 ± 0.1

Data are mean ± SE.

TABLE II
Z AND *C* AT 100 kHz ACROSS GLASS TUBE DURING FLOW OF RBC SUSPENDED IN UNDILUTED PLASMA AT HEMATOCRITS OF 0.3, 0.4, OR 0.5 l/l

	Z	C
0.3 l/l	95.78 ± 4.19 kΩ	0.39 ± 0.01 nF
0.4 l/l	105.86 ± 2.24 kΩ	1.99 ± 0.03 nF
0.5 l/l	121.63 ± 4.48 kΩ	6.06 ± 0.14 nF

Values are mean ± SE of five separate experiments.

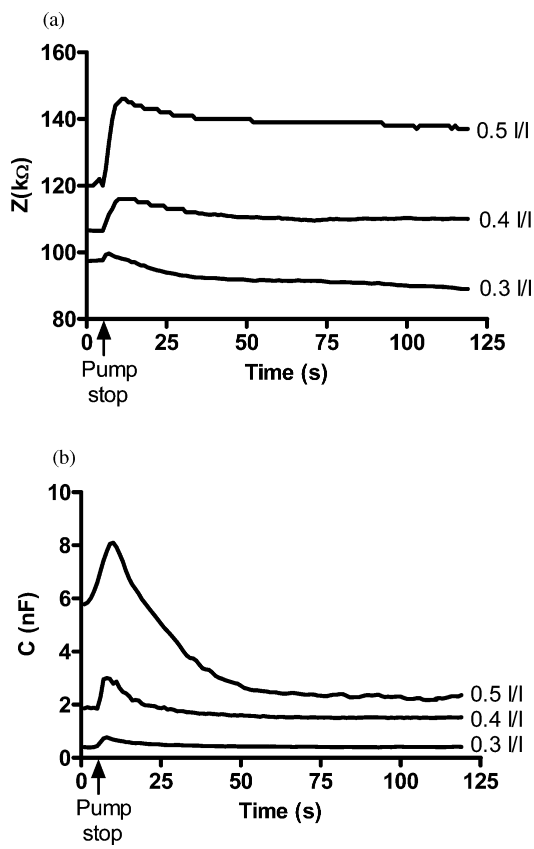

Fig. 6. Time courses of *Z* and *C* of RBC suspended in undiluted plasma at hematocrits of 0.3, 0.4, and 0.5 l/l following flow stoppage in the glass tube. Test signal frequency was 100 kHz.

aggregates were found to increase with increasing hematocrit (see Table II), as predicted by the Maxwell–Fricke equation. The *changes* of *Z* and *C* between flow and after 120 s of stasis were also affected by hematocrit, but exhibited differences (see Fig. 6). If the values during flow and at the last part of the time course (i.e., 100–120 s after flow stoppage) are compared, *Z* was higher in fully aggregated RBC suspensions compared to the disaggregated state for suspensions with 0.4 and 0.5 l/l hematocrit. The difference was more prominent ($\sim$15%) for the suspensions with 0.5 l/l hematocrit, compared to the suspension with 0.4 l/l hematocrit ($\sim$4%). In contrast, the *Z* was lower in fully aggregated RBC suspensions with 0.3 l/l hematocrit compared to the disaggregated state. It should be noted that the level of *Z* and *C* values in aggregated RBC suspensions is determined by both the increase due to shape recovery that defines the starting point for aggregation-related changes and by the magnitude of the decrease following this peak due to aggregation. Obviously, both effects are sensitive to the number of particles in the suspension (i.e., hematocrit), as also predicted by Maxwell–Fricke equation, since hematocrit is the determinant of the influence of "*k*" factor that reflects the geometry and orientation of RBC (according to 1). This hematocrit dependence is especially prominent for 0.3 l/l hematocrit suspensions in which there are very small initial increases due to shape recovery, thus resulting in *Z* and *C* levels at the start of aggregation that are close to the high-flow disaggregated state (see Fig. 6). *C* measurements indicated a different pattern of hematocrit dependence. For suspensions with 0.4 and 0.5 l/l hematocrit, the values for aggregated samples were lower than those measured during flow, with again the difference for 0.5 l/l hematocrit suspensions being significantly greater than for 0.4 l/l. As mentioned earlier, *C* values of aggregated and disaggregated samples were almost identical for 0.3 l/l suspensions.

C. Time Course of LT, Z, and C During RBC Aggregation

Fig. 7 presents typical examples of LT, *Z*, and *C* versus time relations for RBC suspended at 0.4 l/l hematocrit in PBS, in 1/2 and 1/3 diluted plasma, and in undiluted plasma. The LT-time curve for RBC in undiluted plasma [see Fig. 7(a)] exhibited a well-known pattern [21], [22], [25], which reflects the process of RBC aggregation and is qualitatively similar to LT or LR signals obtained via the aggregometers described in Section II-B). There is a sharp decrease in LT following stoppage of flow, which reaches a minimum in a few seconds, followed by increased LT with a characteristic time course [21], [24], [42]. LT-time data for RBC suspended in 1/2 and 1/3 diluted plasma exhibited similar patterns, although the time course was significantly slower in 1/3 diluted plasma and even slower in 1/2 diluted plasma. LT results for RBC suspended in PBS did not exhibit a time course comparable with these recordings and only exhibited progressive decreases with time [see Fig. 7(a)].

Both *Z* and *C* values tended to increase immediately after stoppage of flow, reached a peak, and then, decreased gradually [see Figs. 7(b) and (c)]. Interestingly, the time course for *Z* following the peak value was similar for all RBC suspensions (i.e., plasma, diluted plasma, and PBS), and thus, unlike that observed for LT, the time course of *Z* after the peak was slower compared to LT, even for RBC in undiluted plasma. The time course of *C* after the sudden stop exhibited a different pattern than *Z*: 1) compared to nondiluted plasma, there were smaller peak values and slower decreases of *C* after the peak for RBC

Authorized licensed use limited to: Bezm-i Alem Universitesi. Downloaded on September 22,2025 at 11:42:42 UTC from IEEE Xplore. Restrictions apply.

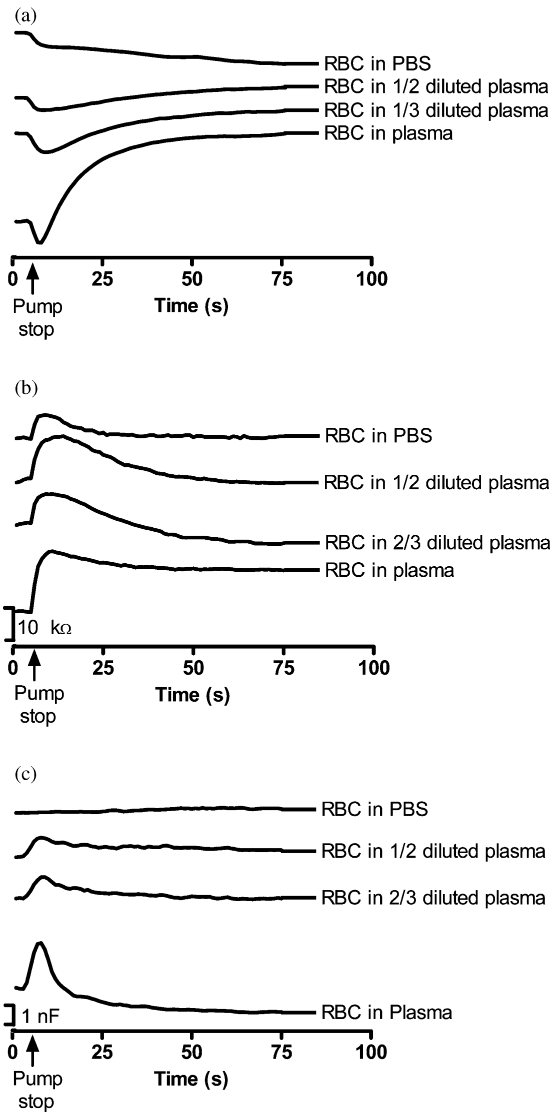

Fig. 7. Time courses of LT, *Z*, and *C* across the glass tube after a sudden stop of flow for RBC suspended in PBS, 1/2 and 1/3 diluted plasma and undiluted plasma. Impedance and capacitance were measured at 100 kHz. (a) Light transmittance. (b) Impedance (*Z*). (c) Capacitance (*C*).

in diluted plasma [see Fig. 7(c)]; and 2) there was no detectable change of *C* for the nonaggregating RBC suspension in PBS.

D. RBC Aggregation Indexes Calculated Using LT, Z, and C Time Courses

Table III presents aggregation parameters calculated as described in Section II-E, using the time courses of LT, *Z*, and *C* after sudden stoppage of flow. It should be noted that the parameter SA is dependent on the numerical value of the recorded modality (LT, *Z*, or *C*), and therefore, the calculated values of SA for different modalities are not comparable. However, it is obvious that SA and AI were calculated, using LT and C data exhibited a similar trend for the diluted plasmas and plasma with 1% dextran 500, with a rank order of plasma + D500 > undiluted plasma > 1/3 diluted plasma > 1/2 diluted plasma. This trend was not seen when using *Z* data (see Table III).

TABLE III
AGGREGATION PARAMETERS REFLECTING EXTENT AND DYNAMICS OF RBC AGGREGATION CALCULATED USING LT, *Z*, AND *C* TIME COURSES AFTER SUDDEN STOP OF FLOW FOR RBC IN UNDILUTED PLASMA, DILUTED PLASMAS, AND PLASMA CONTAINING 1% 500 kDa DEXTRAN (D500)

LT	SA	AI	$T_{1/2}$ (s)
1/2 diluted plasma	12.8 ± 3.5	63.2 ± 3.3	21.5 ± 2.2
1/3 diluted plasma	31.5 ± 3.7	74.1 ± 2.8	16.5 ± 0.6
Plasma	100.6 ± 12.7	78.4 ± 1.5	11.7 ± 1.1
Plasma + 1% D500	153.0 ± 9.9	80.1 ± 1.5	10.8 ± 0.8
Z	SA	AI	$T_{1/2}$
1/2 diluted plasma	253.0 ± 23.3	59.6 ± 1.5	24.0 ± 1.8
1/3 diluted plasma	398.7 ± 18.1	68.7 ± 2.3	16.0 ± 1.9
Plasma	204.3 ± 28.6	73.8 ± 2.5	10.1 ± 0.8
Plasma + 1% D500	207.6 ± 34.2	69.8 ± 5.3	12.2 ± 1.7
C	SA	AI	$T_{1/2}$
1/2 diluted plasma	27.1 ± 1.5	60.6 ± 5.1	21.5 ± 1.0
1/3 diluted plasma	41.2 ± 16.6	67.3 ± 2.8	12.7 ± 2.2
Plasma	81.1 ± 10.6	79.0 ± 1.7	8.8 ± 1.3
Plasma + 1% D500	131.0 ± 17.6	84.4 ± 1.8	10.9 ± 1.2

Z and *C* were monitored at 100 kHz frequency. Data are mean ± SE.

$T_{1/2}$ values based upon LT, *Z*, and *C* data were consistent with slower aggregation for diluted plasma. SA and AI parameters provided by the LORCA aggregometer were in agreement with this sequence. $T_{1/2}$ results via LORCA also indicated slower aggregation for diluted plasma (see Table I).

E. Associations Between Aggregation Indexes

Fig. 8 presents cross-plots of the SA parameter versus the Myrenne aggregometer "M" index for the pooled data obtained, using four types of RBC suspensions (in 1/3 and 1/2 diluted plasma, undiluted plasma, and dextran 500 containing plasma). There were highly significant ($p < 0.001$) correlations for SA values calculated, using LT and *C* data [see Fig. 8(a) and (c)], but not for SA values calculated, using *Z* data [see Fig. 8(b)]. There was also a significant positive correlation between the SA values calculated, using LT and *C* data ($r = 0.68$, $p < 0.0001$), while the correlation between SA values calculated, using LT and *Z* data, was much weaker and negative ($r = -0.40, p < 0.05$) (see Table IV). Other correlation coefficients, including those for AI and $T_{1/2}$, are also presented in Table IV. The relations between AI calculated using *C* or LT data and the M index were also highly significant, whereas AI calculated using *Z* data did not correlate with either the M index or AI based on LT data. Interestingly, $T_{1/2}$ calculated, using *Z* data significantly correlated with both M and $T_{1/2}$ calculated, using LT data, and thus, showed associations similar to that for $T_{1/2}$ based on *C* data. The correlation coefficients of $T_{1/2}$ based on *C* and *Z* versus the M index were negative with *r* larger when using *C* data (see Table IV).

IV. DISCUSSION

Blood is a suspension of cellular elements in plasma, a solution of electrolytes, proteins, and other biomolecules. Although

Authorized licensed use limited to: Bezm-i Alem Universitesi. Downloaded on September 22,2025 at 11:42:42 UTC from IEEE Xplore. Restrictions apply.

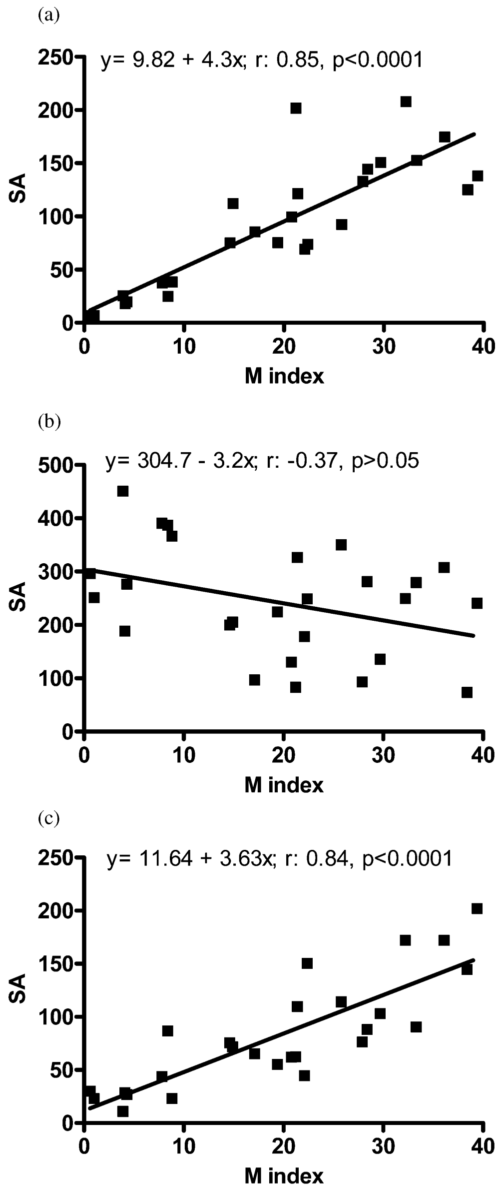

Fig. 8. Linear regression analysis of the relations between the M index and the SA parameter was calculated, using LT, *Z*, and *C* time courses. Data are pooled results for undiluted and diluted plasma and plasma containing 1% 500 kDa dextran (D500). (a) Light transmittance. (b) Impedance (*Z*). (c) Capacitance (*C*).

TABLE IV
PEARSON CORRELATION COEFFICIENTS FOR RELATIONS BETWEEN SA, AI, AND $T_{1/2}$ VALUES CALCULATED USING IMPEDANCE AND CAPACITANCE DATA AND M INDEX. ALSO SHOWN ARE COEFFICIENTS FOR RELATIONS BETWEEN SA, AI AND $T_{1/2}$ VIA LT DATA AND M INDEX

		Impedance	*Capacitance*
SA	M index	-0.37	**0.84*** **
	SA by LT	**-0.40***	**0.68*** **
AI	M index	**0.29**	**0.81*** **
	AI by LT	**0.23**	**0.69*** **
$T_{1/2}$	M index	**-0.67** **	**-0.81*** **
	$T_{1/2}$ by LT	**0.68*** **	**0.69*** **

Statistical significance of correlation coefficients.
*$p < 0.05$.
**$p < 0.01$.
***$p < 0.001$.

its structure seems relatively simple compared to other biological tissues, its physical properties, including flow behavior [43] and electrical properties [5], [6], [8], [9], are complex. RBC constitute over 99% by volume of the cellular elements and are primarily responsible for these complexities. The electrical properties of blood (i.e., *Z* and *C*) are functions of hematocrit and the "effective" geometry of RBC [5], [9], [12], [44], with this geometric term determined by the biological properties of a single cell (e.g., geometry and deformability), by external factors (e.g., shear forces) and by intercellular interactions (e.g., aggregate formation resulting in increased particle size and altered particle geometry). This study confirmed the dependence of *Z* and *C* on hematocrit and shape change/orientation due to flow as suggested by earlier theoretical and experimental studies [8], [9], [32], [45]. Alterations of both *Z* and *C* were observed during the transition from flow to stasis in which two important changes occur in "effective" geometry: 1) the initial phase of increased *Z* and *C* reflects the recovery of RBC morphology for cells initially deformed by shear forces during high-shear flow (corresponding to $\sim$500 s^{-1} shear rate), with the shape changing from an elongated form to the normal biconcave-discoid shape [46]–[48]; and 2) the later phase of gradual decreases of *Z* and *C* reflects RBC aggregate formation, which follows a characteristic time course [17].

It should be noted that this study differs from previous reports owing to its focus on the analysis of the time course of electrical properties of RBC suspensions during the transition from flow to stasis, rather than focusing on measurement of electrical properties at stasis or at various constant flow rates. The transition phase is known to carry important information related to RBC aggregation behavior [20]. It also differs by using a cylindrical test chamber to measure *Z* and *C* in the direction of flow across a glass tube filled with a RBC suspension. One millimeter diameter glass tube was selected in order to avoid wall effects [49], and stainless steel tube electrodes were placed at the two ends of the 75 mm long glass tube. At frequencies below 500 kHz, the *Z* across the tube was $\sim$40 kΩ when filled with PBS, $\sim$50 kΩ when filled with plasma, and above 100 kΩ when filled with RBC suspension at 0.4 l/l hematocrit (see Fig. 3). Most previous studies have employed rectangular or cylindrical flow chambers and electrodes with various orientations (e.g., parallel), the measured *Z* for blood with such chambers was far below the values obtained in this study [32], [33]. The higher *Z* of the tube served to reduce the relative contribution of artifacts due to technical issues, such as electrode polarization, the two-electrode configuration used herein may also have contributed to the high *Z* characterizing the measurement system.

The test signal used in this study (i.e., 1 V) and the high *Z* of the tube resulted in currents on the order of 10 μA, when the tube was filled with RBC suspensions, and thus, this current is below the range where current density may interfere with *Z* and *C* measurements [9]. Furthermore, the large surface area of the electrodes used in this study also reduced the current density at electrode–suspension interfaces, thus tending to minimize electrode effects. The cylindrical flow chamber geometry allowed measurement of electrical properties of RBC suspensions, using a two-electrode configuration rather than a four-electrode

Authorized licensed use limited to: Bezm-i Alem Universitesi. Downloaded on September 22,2025 at 11:42:42 UTC from IEEE Xplore. Restrictions apply.

arrangement. While it has been shown that a four-electrode system is superior to a two-electrode system at frequencies below 20 kHz, both arrangements are equally effective for the frequency range used in this study [31].

Since the *C* of the RBC suspensions were derived from the *Z* measured at 100 kHz, using an LCR meter as previously used by other investigators [5], [32], the resulting *C* values did not exactly reflect RBC membrane capacitance (i.e., C_m in the three-element model of blood bioimpedance, Fig. 1), but are expected to be strongly influenced by this membrane property. Zhao *et al.* have reported a method to calculate C_m based on impedance measurements at three signal frequencies within the β-dispersion range [10]. However, this approach was not applicable for our dynamic measurements during the transition from flow to stasis, since simultaneous measurements at different frequencies were not possible with the present system. Further, preliminary studies using different frequencies for separate measurements of the time course of *Z* with the same sample indicated slight differences in aggregation response or measurement conditions (e.g., electrode characteristics), calculation of C_m using such multifrequency data was thus also not possible.

The difference of *Z* and *C* values measured during flow (i.e., fully disaggregated state) and at stasis (i.e., after the full development of RBC aggregation) was strongly hematocrit dependent (see Fig. 6). In addition, the pattern and magnitude of alterations during the transition period were also markedly affected by hematocrit (see Fig. 6). Both *Z* and *C* exhibited a sudden increment immediately after flow stoppage, reached a maximum within a few seconds, and then, began to decline. In addition to the obvious differences in the magnitude of the changes, the time course of these changes also appeared to be hematocrit dependent. This influence of hematocrit can, at least in part, be explained by the well-known influence of hematocrit on RBC aggregation kinetics [21], [23], [42], [50]. It thus seems logical to assume that the time course of *C* and *Z* during the transition from flow to stasis should reflect the time course of RBC aggregation. LT through RBC suspensions is well-known to reflect RBC aggregation [21], [22], [27], and includes an abrupt change due to RBC shape recovery followed by increased LT due to the decreased number of individual particles accompanying increased effective particle size (see Fig. 4). Although the changes of *Z* and *C* corresponding to shape recovery and aggregation are opposite in sign, their overall behavior are consistent with LT results (see Figs. 6 and 7).

An unexpected finding of this study was the time course of *Z* changes for nonaggregating suspensions of RBC in PBS [see Fig. 7(b)]. *Z* changes had the same pattern as those for aggregating suspensions, while such similarity between aggregating and nonaggregating suspensions was not observed for LT and *C*. Note that the lack of detectable aggregation in RBC–PBS suspensions was confirmed by the contrasting time courses of LT and *C* measured simultaneously with *Z* (see Fig. 7). The initial phase of increased *Z* of RBC suspensions in PBS following flow stoppage can be explained by the shape recovery-disorientation process. However, the time constant of this process is within several hundred milliseconds [46] and cannot be expected to have an influence after this initial phase of a few seconds. This finding is in conflict with the reports of Pribush *et al.* [33] and Antonova *et al.* [30], and Antonova and Rhia [51], who suggest the aggregation process is reflected by the time course of electrical conductance after the cessation of flow. However, experimental conditions differed between these prior reports and tis study: 1) the measurement chamber geometry in both prior studies was not a cylindrical glass tube. Pribush *et al*. measured *Z*, using two parallel electrodes separated by 2 mm, with the electrode axis perpendicular to the flow axis [33]. Antonova *et al*. used a Couette-type viscometer with platinum electrodes attached to the surfaces of the cup [51]; 2) Pribush *et al.* measured conductances at 200 kHz [33], while Antonova *et al.* used 2 kHz [30], [51]; and 3) no prior study reported results for suspensions of normal RBC in a nonaggregating suspending media. The *Z* change of nonaggregating RBC suspensions cannot be explained by current experimental evidence and available literature data, and it is not yet clear if this behavior is limited to the particular flow-measurement chamber geometry used in this study.

In addition to the unexpected *Z* findings for nonaggregating RBC suspensions, *Z* measurements also failed to correctly reflect altered aggregation induced by plasma dilution or 500 kDa dextran, whereas these alterations were detected by LT and *C* (see Fig. 7 and Table III). Visual inspection of LT and *C* curves for RBC suspensions with 1/3 or 1/2 diluted plasma indicate that both overall changes and the rate of change were significantly decreased by plasma dilution. Analysis of LT and *C* curves indicated, decreased SA and AI aggregation parameters and increased aggregation half time (see Table III). These alterations of RBC aggregation in diluted plasma or plasma $+$ 1% dextran D500 were confirmed by measurements, using commercial instruments designed to quantitate RBC aggregation (see Fig. 5 and Table I). Linear regression analysis and Pearson correlation coefficients also support the merit of LT and *C* measurements, with significant positive correlations between SA computed from LT and *C* data and the M index of the Myrenne aggregometer [24]. SA was calculated using *Z* data did not correlate with the M index. These observations suggest that the time course of *Z* following stoppage of flow in the cylindrical glass tube is affected by flow-related phenomena that may include, but are not limited to, shear-induced changes in adsorption of macromolecules on electrodes, partial blockage of the interface by adhesion of the dispersed particles [33].

Based upon the discussion aforementioned, our results strongly suggest that capacitance is the preferred electrical parameter to monitor aggregation properties of RBC suspensions. It should be noted that capacitance values obtained in this study are expected to reflect the membrane capacitance of RBC. While merely speculative, it is interesting to consider the observed decrement of *C* with RBC aggregation in light of the morphology of RBC aggregates: RBC–RBC form face-to-face structures with parallel membrane surfaces (i.e, rouleaux formation). As a result, the membrane capacitance of each cell is in series in aggregates, resulting in a lower equivalent capacitance as RBC aggregation progresses.

The correlations between LT- and C-based parameters versus the M index were comparable (see Table IV), thereby suggesting

Authorized licensed use limited to: Bezm-i Alem Universitesi. Downloaded on September 22,2025 at 11:42:42 UTC from IEEE Xplore. Restrictions apply.

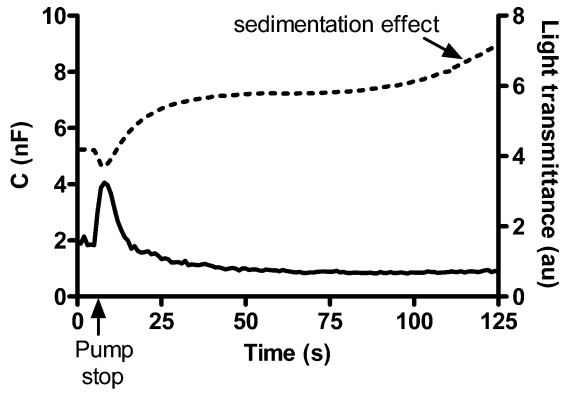

Fig. 9. Simultaneous recordings of LT (. . .) and series capacitance (—) following sudden stoppage of flow for a normal blood sample with 0.4 l/l hematocrit. The increment of LT during later part of the record (∼90 s after the flow stop) reflects RBC sedimentation which does not affect capacitance.

equal usefulness of these two modalities for evaluating RBC aggregation. However, in our system (i.e., horizontal glass tube with LT monitored in a horizontal direction), the LT parameter was sensitive to RBC sedimentation, which started to be evident after ∼75 s (see Fig. 9). In contrast, *C* recorded simultaneously was not affected by sedimentation, yet was similarly sensitive to the aggregation process (see Fig. 9), and thus, this insensitivity to sedimentation should be regarded as an advantage for the *C* measurements.

In overview, our results indicate that RBC aggregation parameters based upon *C* data obtained during the transition from flow to stasis are in general agreement with those derived from LT data and with RBC aggregation indexes measured, using commercial instruments. Parameters based on *C* data were more robust and had much stronger correlations with the generally accepted indexes. Aggregation parameters were calculated, using *Z* time course data often failed to correlate with known changes of aggregation, even incorrectly indicating aggregation for cells in nonaggregating media (i.e., RBC in PBS). Differences between our results using a horizontal tube and other studies using different chamber geometries, as well as the bases for the failure of *Z* time course reflecting RBC aggregation, clearly warrant further studies.

References

[1] C. Balan, C. Balut, L. Gheorghe, C. Gheorghe, E. Gheorghiu, and G. Ursu, “Experimental determination of blood permittivity and conductivity in simple shear flow,” *Clin. Hemorheol. Microcirc.*, vol. 30, pp. 359–364, 2004.

[2] M. Sosa, J. B. Bernal-Alvarado, M. Jimenez-Moreno, J. C. Hernandez, G. Gutierrez-Jarez, M. Vargas-Luna, R. Huerta, J. C. Villagomez-Castro, and P. Palomares, “Magnetic field influence on electrical properties of human blood measured by impedance spectroscopy,” *Bioelectromagnetics*, vol. 26, pp. 564–570, 2005.

[3] Y. Ulgen and M. Sezdi, “Physiological quality assessment of stored whole blood by means of electrical measurements,” *Med. Biol. Eng. Comput.*, vol. 45, pp. 653–660, 2007.

[4] G. A. M. Pop, W. J. Hop, M. van der Jagt, J. Quak, D. Dekkers, Z. Chang, F. J. Gijsen, D. J. Dunncker, and C. J. Slager, “Blood electrical impedance closely matches whole blood viscosity as parameter of hemorheology and inflammation,” *Appl. Rheol.*, vol. 13, pp. 305–312, 2003.

[5] H. Beving, L. E. G. Eriksson, C. L. Davey, and D. B. Kell, “Dielectric properties of human blood and erythrocytes at radio frequencies (0.2–10 MHz); dependence on cell volume fraction and medium composition,” *Eur. Biophys. J.*, vol. 23, pp. 207–215, 1994.

[6] T. X. Zhao and B. Jacobson, “Quantitative correlations among fibrinogen concentration, sedimentation rate and electrical impedance of blood,” *Med. Biol. Eng. Comput.*, vol. 35, pp. 181–185, 1997.

[7] H. Fricke, “The Maxwell–Wagner dispersion in a suspension of ellipsoids,” *J. Phys. Chem.*, vol. 57, pp. 934–937, 1953.

[8] R. L. Gaw, B. H. Cornish, and B. J. Thomas, “The electrical impedance of pulsatile blood flowing through rigid tubes: A theoretical investigation,” *IEEE Trans. Biomed. Eng.*, vol. 55, no. 2, pp. 721–727, Feb. 2008.

[9] A. E. Hoetink, Th. J. C. Faes, K. R. Visser, and R. M. Heethaar, “On the flow dependency of the electrical conductivity of blood,” *IEEE Trans. Biomed. Eng.*, vol. 51, no. 7, pp. 1251–1261, Jul. 2004.

[10] T. X. Zhao, B. Jacobson, and T. Ribbe, “Triple-frequency method for measuring blood impedance,” *Physiol. Meas.*, vol. 14, no. 2, pp. 145–156, 1993.

[11] H. Fricke and S. Morse, “The electrical resistance and capacity of blood for frequencies between 800 and 4.5 million cycles,” *J. Gen. Physiol.*, vol. 9, pp. 153–167, 1925.

[12] H. Fricke, “The electrical capacity of suspensions with special reference to blood,” *J. Gen. Physiol.*, vol. 9, pp. 137–152, 1925.

[13] H. Fricke, “A mathematical treatment of the electrical conductivity and capacity of disperse systems,” *Phys. Rev.*, vol. 4, pp. 575–587, 1924.

[14] L. A. Geddes and C. Sadler, “The specific resistance of blood at body temperature,” *Med. Biol. Eng.*, vol. 11, pp. 336–339, 1973.

[15] S. Chien, “Red cell deformability and its relevance to blood flow,” *Ann. Rev. Physiol.*, vol. 49, pp. 177–192, 1987.

[16] O. K. Baskurt and H. J. Meiselman, “Blood rheology and hemodynamics,” *Semin. Thromb. Hemost.*, vol. 29, no. 5, pp. 435–450, Oct. 2003.

[17] B. Neu and H. J. Meiselman, “Red blood cell aggregation,” in *Handbook of Hemorheology and Hemodynamics*, O. K. Baskurt, M. R. Hardeman, M. W. Rampling, and H. J. Meiselman, Eds. Amsterdam, The Netherlands: IOS Press, 2007, pp. 114–136.

[18] O. K. Baskurt, “In vivo correlates of altered blood rheology,” *Biorheology*, vol. 45, pp. 629–638, 2008.

[19] O. K. Baskurt, “Mechanisms of blood rheology alterations,” in *Handbook of Hemorheology and Hemodynamics*, O. K. Baskurt, M. R. Hardeman, M. W. Rampling, and H. J. Meiselman, Eds. Amsterdam, The Netherlands: IOS Press, 2007, pp. 170–190.

[20] M. R. Hardeman, P. T. Goedhart, and S. Shin, “Methods in hemorheology,” in *Handbook Hemorheology and Hemodynamics*, O. K. Baskurt, M. R. Hardeman, M. W. Rampling, and H. J. Meiselman, Eds. Amsterdam, The Netherlands: IOS Press, 2007, pp. 242–266.

[21] O. K. Baskurt, H. J. Meiselman, and E. Kayar, “Measurement of red blood cell aggregation in a “plate-plate” shearing system by analysis of light transmission,” *Clin. Hemorheol. Microcirc.*, vol. 19, no. 4, pp. 307–314, Dec. 1998.

[22] A. Gaspar-Rosas and G. B. Thurston, “Erythrocyte aggregate rheology by transmitted and reflected light,” *Biorheology*, vol. 25, pp. 471–487, 1988.

[23] M. R. Hardeman, J. G. G. Dobbe, and C. Ince, “The laser-assisted optical rotational cell analyzer (LORCA) as red blood cell aggregometer,” *Clin. Hemorheol. Microcir.*, vol. 25, no. 1, pp. 1–11, 2001.

[24] H. Kiesewetter, H. Radtke, R. Schneider, K. Mussler, A. Scheffler, and H. Schmid-Schonbein, “The mini erythrocyte aggregometer: A new apparatus for the rapid quantification of the extent of erythrocyte aggregation,” *Biomed. Tech. (Berlin)*, vol. 28, pp. 209–213, 1982.

[25] S. Shin, Y. Yang, and J. S. Suh, “Measurement of erythrocyte aggregation in a microchip-based stirring-system by analysis of light transmission and backscattering,” *Biorheology*, vol. 45, no. 1–2, pp. 71–72, 2008.

[26] W. G. Zijlstra, “Syllectometry, a new method for studying rouleaux formation of red blood cells,” *Acta Phys. Pharm. Neerl.*, vol. 7, pp. 153–154, 1958.

[27] H. Schmid-Schoenbein, J. von Gosen, L. Heinich, H. J. Klose, and E. Volger, “A counter-rotating “rheoscope chamber” for the study of the microrheology of blood cell aggregation by microscopic observation and microphotometry,” *Microvasc. Res.*, vol. 6, pp. 366–376, 1973.

[28] R. M. Bauersachs, R. B. Wenby, and H. J. Meiselman, “Determination of specific red blood cell aggregation indices via an automated system,” *Clin. Hemorheol.*, vol. 9, pp. 1–25, 1989.

[29] O. K. Baskurt, M. Uyuklu, P. Ulker, M. Cengiz, N. Nemeth, T. Alexy, S. Shin, M. R. Hardeman, and H. J. Meiselman, “Comparison of three instruments for measuring red blood cell aggregation,” *Clin. Hemorheol. Microcirc.*, vol. 43, pp. 283–298, 2009.

[30] N. Antonova, P. Riha, and I. Ivanov, “Time dependent variation of human blood conductivity as a method for an estimation of RBC aggregation,” *Clin. Hemorheol. Microcirc.*, vol. 39, pp. 69–78, 2008.

Authorized licensed use limited to: Bezm-i Alem Universitesi. Downloaded on September 22,2025 at 11:42:42 UTC from IEEE Xplore. Restrictions apply.

[31] Z. Chang, G. A. M. Pop, and G. C. M. Meijer, "A comparison of two and four electrode techniques to characterize blood impedance for the frequency range of 100 Hz to 100 MHz," *IEEE Trans. Biomed. Eng.*, vol. 55, no. 3, pp. 1247–1249, Mar. 2008.

[32] A. Pribush, H. J. Meiselman, D. Meyerstein, and N. Meyerstein, "Dielectric approach to the investigation of erythrocyte aggregation. Part I. Experimental basis of the method," *Biorheology*, vol. 36, no. 5–6, pp. 411–423, 1999.

[33] A. Pribush, D. Meyerstein, and N. Meyerstein, "Conductometric study of shear-dependent processes in red cell suspensions. I. Effect of red blood cell aggregate morphology on blood conductance," *Biorheology*, vol. 41, no. 1, pp. 13–28, 2004.

[34] A. Pribush, L. Hatzkelson, D. Meyerstein, and N. Meyerstein, "A novel technique for quantification of erythrocyte aggregation abnormalities in pathophysiological situations," *Clin. Hemorheol. Microcirc.*, vol. 36, pp. 121–132, 2007.

[35] O. K. Baskurt, M. Uyuklu, and H. J. Meiselman, "Simultaneous monitoring of electrical conductance and light transmittance during red blood cell aggregation," *Biorheology*, vol. 46, pp. 239–249, 2009.

[36] O. K. Baskurt, M. Boynard, G. R. Cokelet, P. Connes, B. M. Cooke, S. Forconi, F. Liao, M. R. Hardeman, F. Jung, H. J. Meiselman, G. B. Nash, N. Nemeth, B. Neu, B. Sandhagen, S. Shin, G. B. Thurston, and J. L. Wautier, "New guidelines for hemorheological laboratory techniques," *Clin. Hemorheol. Microcir.*, vol. 42, pp. 75–97, 2009.

[37] S. Chien, "Biophysical behaviour of red cells in suspensions," in *The Red Blood Cell*, 2nd ed., D. M. Surgenor, Ed. New York: Academic, 1975, pp. 1031–1133.

[38] O. K. Baskurt, M. Bor-Kucukatay, O. Yalcin, H. J. Meiselman, and J. K. Armstrong, "Standard aggregating media to test the "aggregability" of rat red blood cells," *Clin. Hemorheol. Microcirc.*, vol. 22, no. 2, pp. 161–166, 2000.

[39] *Instruction Manual 3532-50 LCR Hitester*, Hioki EE Corp., Nagano, Japan, 2006, pp. 1–180.

[40] D. Holder, "Brief introduction to bioimpedance," in *Electrical Impedance Tomography*. Boca Raton, FL: CRC Press, 2005, pp. 411–422.

[41] T. W. Secomb and A. R. Pries, "Basic principles of hemodynamics," in *Handbook of Hemorheology and Hemodynamics*, O. K. Baskurt, M. R. Hardeman, M. W. Rampling, and H. J. Meiselman, Eds. Amsterdam, The Netherlands: IOS Press, 2007, pp. 289–306.

[42] S. Shin, Y. Yang, and J. S. Suh, "Measurement of erythrocyte aggregation in a microchip-based stirring system by light transmission," *Clin. Hemorheol. Microcirc.*, vol. 41, pp. 197–207, 2009.

[43] G. R. Cokelet and H. J. Meiselman, "Macro and microrheological properties of blood," in *Handbook of Hemorheology and Hemodynamics*, O. K. Baskurt, M. R. Hardeman, M. W. Rampling, and H. J. Meiselman, Eds. Amsterdam, The Netherlands: IOS Press, 2007, pp. 45–71.

[44] H. Fricke, "Relation of the permittivity of biological cell suspensions to fractional cell volume," *Nature*, vol. 172, no. 4381, pp. 731–732, 1953.

[45] A. Pribush, H. J. Meiselman, D. Meyerstein, and N. Meyerstein, "Dielectric approach to investigation of erythrocyte aggregation. II. Kinetics of erythrocyte aggregation-disaggregation in quiescent and flowing blood," *Biorheology*, vol. 37, no. 5–6, pp. 429–441, 2000.

[46] O. K. Baskurt and H. J. Meiselman, "Determination of red blood cell shape recovery time constant in a Couette system by the analysis of light reflectance and ektacytometry," *Biorheology*, vol. 33, no. 6, pp. 489–503, Nov. 1996.

[47] R. M. Hochmuth, "Deformability and viscoelasticity of human erythrocyte membrane," *Scand. J. Clin. Lab. Invest.*, vol. 41, pp. 63–66, 1981.

[48] S. P. Sutera, E. R. Mueller, and G. I. Zahalak, "Extensional recovery of an intact erythrocyte from a tank-treading motion," *J. Biomech. Eng.*, vol. 112, pp. 250–256, 1990.

[49] H. A. Barnes, "A review of the slip (wall depletion) of polymer solutions, emulsions and particle suspensions in viscometers: Its cause, character and cure," *J. Non-Newtonian Fluid Mech.*, vol. 56, pp. 221–251, 1995.

[50] L. H. Deng, J. C. Barbenel, and G. D. O. Lowe, "Influence of hematocrit on erythrocyte aggregation kinetics for suspensions of red blood cells in autologous plasma," *Biorheology*, vol. 31, pp. 193–205, 1994.

[51] N. Antonova and P. Riha, "Studies of electrorheological properties of blood," *Clin. Hemorheol. Microcirc.*, vol. 35, pp. 19–29, 2006.

Oguz K. Baskurt was born in Istanbul, Turkey, in 1956. He received the M.D. and Ph.D. degrees in physiology from Hacettepe University, Ankara, Turkey.

He is currently engaged as a Professor with the Department of Physiology, Faculty of Medicine, Akdeniz University, Antalya. He conducted extensive research mostly in the fields of red blood cell aggregation, comparative hemorheology, and *in vivo* hemorheology. He has authored or coauthored more than 150 papers, mostly in international and peer-reviewed journals. He is author of a book entitled *Handbook of Hemorheology and Hemodynamics*. His current research interests include the rheological properties of blood and their physiological significance.

Dr. Baskurt was the President of the International Society for Clinical Hemorheology from 1999 to 2005. He is on the editorial boards of several international journals.

Mehmet Uyuklu was born in Kahramanmaraş, Turkey, in 1977. He received the M.S. degree in physiology from the Akdeniz University, Antalya, Turkey, in 2006, where he is working toward the Ph.D. degree in the Department of Physiology, Faculty of Medicine.

He is currently engaged as a Research Assistant with the Department of Physiology, Faculty of Medicine. His research interests include red blood cell aggregation, importance of red blood cell factors in aggregation, role of hemorheological factors in hemodynamics, hemorheological instrumentation, and comparative hemorheology.

Herbert J. Meiselman was born in Jamestown, NY, in 1940. He received the Sc.D. degree in chemical engineering from the Massachusetts Institute of Technology, Cambridge.

He is currently a Professor and a Vice-Chair with the Department of Physiology and Biophysics, Keck School of Medicine, Los Angeles, CA. His research interests include the physicochemical and rheological properties of blood and its cellular components: normal and pathologic blood, cell mechanics, the mechanism or red cell aggregation, and comparative studies of various mammalian species. He has authored or coauthored more than 250 peer-review papers and has edited three books including the *Handbook of Hemorheology and Hemodynamics*.

Dr. Meiselman is currently a President of the International Society of Clinical Hemorheology and engaged on the Editorial Board of Biorheology and Clinical Hemorheology and Microcirculation.

Authorized licensed use limited to: Bezm-i Alem Universitesi. Downloaded on September 22,2025 at 11:42:42 UTC from IEEE Xplore. Restrictions apply.